sults of figure 3.11 for the top faces. The discontinuity appears in all its evidence: along the row of elements with tensile stress equal to 827 MPa there is an upside-down element that presents the correct absolute value for the stress, but of compression instead of traction. Contrary to what happens for the discordant orientations seen in § 3.3, in this case it is not possible to "correct" the graphic representation simply by choosing a different reference system, because top and bottom are associated with the element and its definition. A contour averaged in the nodes, as seen, would have slightly hidden this effect, making its identification more difficult.

In addition to the bending regime for shell elements there is also the membrane regime; the stress state associated with it is displayed by plotting the stress in the middle plane of the elements (called middle surface). In this case, given the lack of loads with components parallel to the plate plane, the membrane regime does not exist and the plate works in pure bending. It is worth highlighting the fact that, should we be in the presence of large deformations, the calculation should be of non-linear type and in this case, depending on the constraint conditions, membrane components may arise, as we will see in Chapter 11.

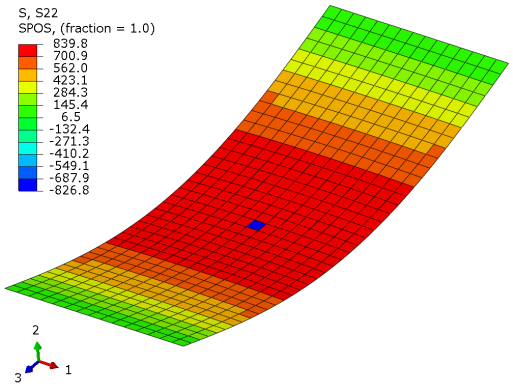

Figure 3.11. Contour of the (un-averaged) stress in the longitudinal direction. It is possible to observe the discontinuity due to the tilting of one element with respect to the others.

3.4.2 Intersections among elements located on different planes

We see, through an other example, an additional problem that can be found in the post-processing of the results on shell element models: we consider the double T beam shown in figure 3.12 through its shell type finite element model; in the figure are also contained the dimensions of the section. The beam is clamped at one end and loaded at the other end by a vertical force F = 10000 N that submits it to bending and shear.

Since the force lies in the plane of the web, the web will work exclusively in the membrane regime, while the two flanges will see both the membrane, preponderant, and flexural contributions. To avoid having to deal with local overstress due to the discontinuity caused by the constraints, we will focus on analyzing the results in the centerline section.

Let's start with the stresses generated by bending by going to determine the values of the stresses at the points shown in figure 3.13, first with the methods of Solid Mechanics and then through the finite element model.

$$\sigma_A = \frac{M_{bmid}}{I} \cdot \frac{h_A}{2} = 161.8 \text{ MPa} \qquad \sigma_B = \sigma_C = \frac{M_{bmid}}{I} \cdot \frac{h_B}{2} = 152.1 \text{ MPa}$$

being:

$$M_{bmid} = F \cdot \frac{L}{2} = 2500000 \text{ Nmm} \qquad I = 772366 \text{ mm}^4$$

$$h_A = 100 \text{ mm} \qquad h_B = 97 \text{ mm}$$

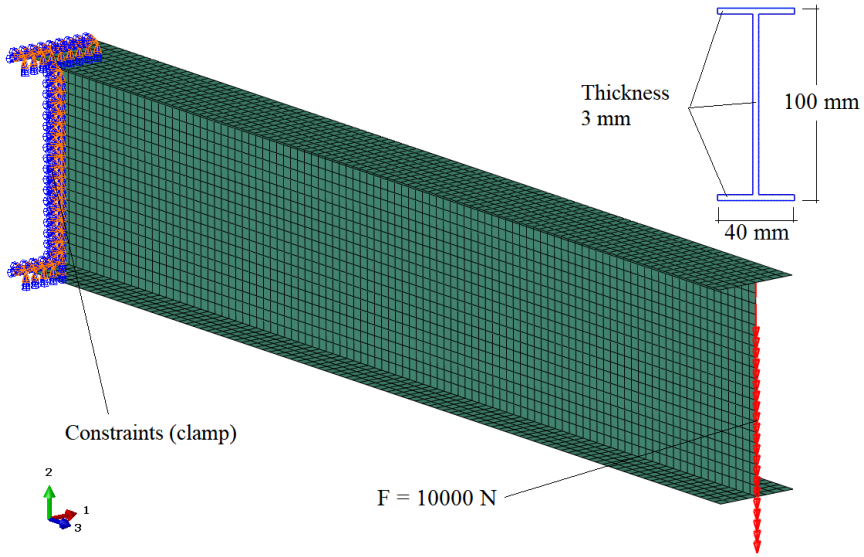

Figure 3.12. The beam has a length L = 500 mm. The shell elements lie in the middle planes of the web and the flange.

In figure 3.14 we show the contour of the longitudinal stress for the top faces which, in the case of the top flange, is the value to be compared with σ_A, while figure 3.15 shows the distribution of the longitudinal stress for the bottom faces, to be clearly compared with σ_B and σ_C.

In both cases the error made is very small, around 1÷2%.

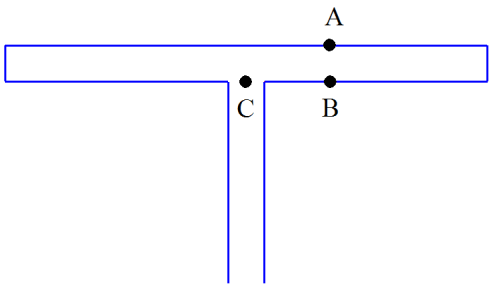

Figure 3.13. Points of investigation of the stress state induced by bending.

We observe that while in the theoretical case σ_B and σ_C coincide because the distance from the neutral axis is equal in both conditions, in the finite element model there is a difference, small but still appreciable.

This happens because at point C of the model, the stress, averaged, also takes into account the contribution of the web element that enters the flange. But why is the value higher? Investigating in the numerical results (e.g., by clicking with the mouse on an un-averaged plotting), one observes that in the elements of the flange at the intersection with the web there is exactly the same value as for σ_B, as shown in figure 3.16. Therefore, since the average is higher, the responsible party can only be the web ele-

ment; in fact, observing figure 3.16, we see that in that element the tension is 154.4 MPa. We recall that shell element models, generally, are constructed by laying the elements in the middle plane of the surfaces; in this example, therefore, the web does not have a height of $(100-2\cdot3)=94$ mm but of $(100-2\cdot1.5)=97$ mm. Therefore the model " picks up ", in the core, a stress equal to:

$$\sigma_{CFEM}=\frac{M_{fmez}}{I}\cdot\frac{97}{2}=156.9\ \text{MPa}$$

with an error still around 1.5% with respect to the theoretical value, but in line with what was found for the other two points far from the intersection with the web.

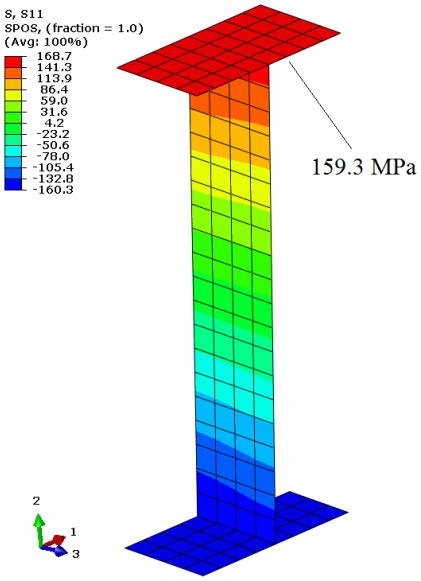

Figure 3.14. Longitudinal stress in the beam centerline: top faces.

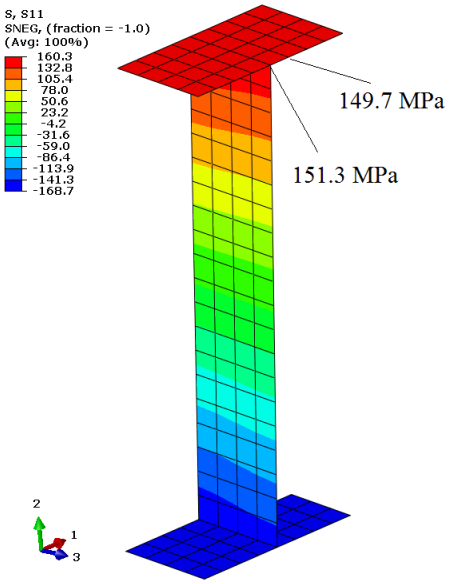

Figure 3.15. Longitudinal stress in the beam centerline: bottom faces.

This effect is more evident the higher the thicknesses are, even if in a shell model the thicknesses should not be too high compared to the other dimensions of the structure. In this simple case it is easy to understand that the correct value to be taken is the one given by the elements of the flange, while in other occasions to discriminate could be more difficult.

Let us now examine the stresses generated by the shear. The shear force is constant along the axis of the beam, so we could analyze any section (apart from the constrained section for the already mentioned discontinuity problems); we will therefore focus again on the section in the middle.

Solid Mechanics tells us that the maximum shear stress is located at the centroid axis and is equal to:

$$\tau_{max} = \frac{F \cdot S^*}{I \cdot b} = -39.4\,\text{MPa}$$

being $S^* = 9132.4\ \text{mm}^3$ the static moment, for the definition of which we refer to Solid Mechanics texts, and b = 3 mm the thickness of the web.

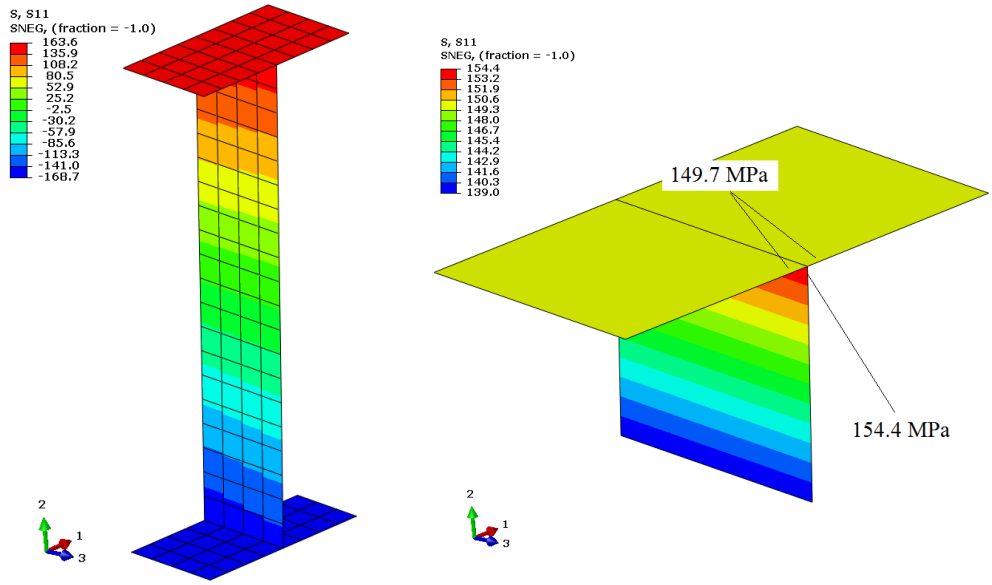

Figure 3.16. Longitudinal (un-averaged) stress in the middle of the beam: bottom faces. An enlargement is also reported with the values, in the interface node, of the stress in the flange and web elements.

We then know that the τ are not null in the flange, but they can be calculated with the same formula, substituting the appropriate values of S^* and of b. For example, in the flange and at 15 mm from the edge, we obtain a value of ±9.4 MPa (the sign depends on which part of the web is considered).

In figure 3.17 it is shown the contour of the shear stress in the middle section. In correspondence of the centroid axis the value that is recorded in the model is equal to -39.2 MPa, while in the flanges it is equal to ±9.3 MPa; in both locations the values practically coincide with the theory, as it can be found from figure 3.17.

Let's spend a few more words on this example, in particular on the membrane stress state, i.e. the one related to the middle plane of the shell elements. We said that the web works in a purely membrane regime, exactly like the beam in figure 3.1, while the flanges will also have a minimal bending contribution.

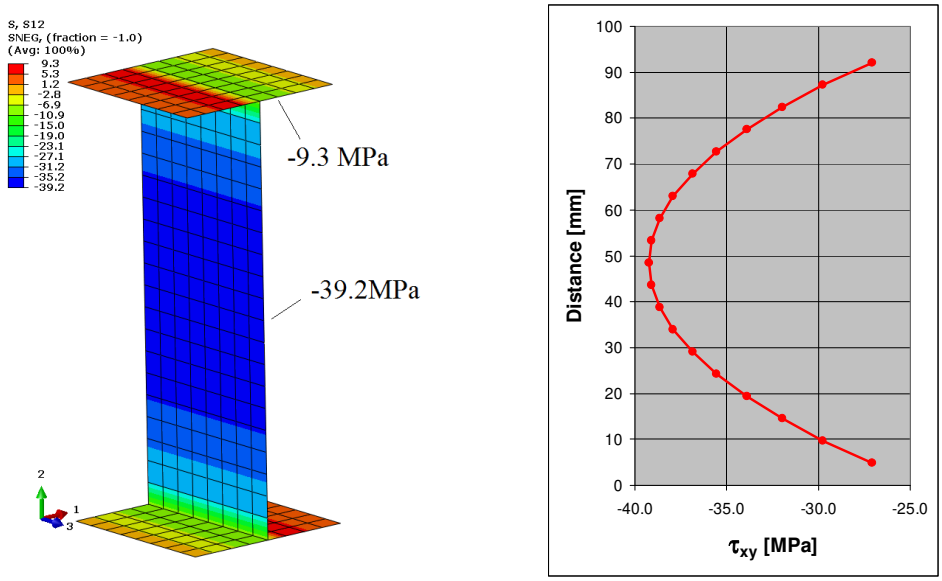

Figure 3.17. Shear stress contour. Both in the web and in the flanges, the agreement with the theory is definitely good. In the right part, the contour of the shear stress along the web is shown, which, as we know, is parabolic.

The value of the membrane stress can be calculated as the average of the stresses at the top and bottom faces; therefore, we can determine it from figures 3.14 and 3.15 (for a point halfway between A and B - see figure 3.13) as:

$$\sigma_{mem} = \frac{159.3+149.7}{2} = 154.5\,\text{MPa}$$

We observe that the bending contribution is therefore ± 4.8 MPa.

Figure 3.18 shows the contour of the longitudinal stress evaluated in the middle plane, which represents precisely the membrane regime.

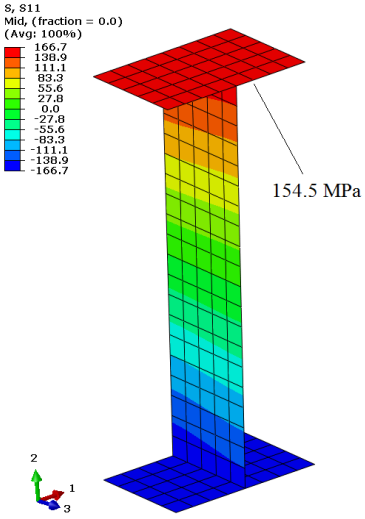

Figure 3.18. Longitudinal stress contour in the middle plane.

3.4.3 Discontinuous joints

We mentioned in Chapter 1 the connection systems between parts of the same structure modeled with shell elements; let's now see how to deal with this issue when the connection system involves discrete points. Let us have, for example, the beam made with three plates connected together, as represented in figure 3.19; the structure is